

# A Hybrid Generative and Discriminative PointNet on Unordered Point Sets

Yang Ye

Department of Computer Science  
Georgia State University  
Atlanta, GA 30302, USA  
yye10@student.gsu.edu

Shihao Ji

Department of Computer Science  
Georgia State University  
Atlanta, GA 30302, USA  
sji@gsu.edu

## Abstract

As point cloud provides a natural and flexible representation usable in myriad applications (e.g., robotics and self-driving cars), the ability to synthesize point clouds for analysis becomes crucial. Recently, Xie et al. [65] propose a generative model for unordered point sets in the form of an energy-based model (EBM). Despite the model achieving an impressive performance for point cloud generation, one separate model needs to be trained for each category to capture the complex point set distributions. Besides, their method is unable to classify point clouds directly and requires additional fine-tuning for classification. One interesting question is: Can we train a single network for a hybrid generative and discriminative model of point clouds? A similar question has recently been answered in the affirmative for images, introducing the framework of Joint Energy-based Model (JEM) [13, 68], which achieves high performance in image classification and generation simultaneously. This paper proposes GDPNet, the first hybrid Generative and Discriminative PointNet that extends JEM for point cloud classification and generation. Our GDPNet retains strong discriminative power of modern PointNet classifiers [42], while generating point cloud samples rivaling state-of-the-art generative approaches.

## 1. Introduction

With the rapid development of 3D sensing devices (e.g., LiDAR and RGB-D camera), a huge amount of point cloud data are collected in the area of robotics, autonomous driving and virtual reality [10, 39, 40]. A 3D point cloud, composed of the raw coordinates of scanned points in 3D space, is an accurate representation of an object or shape and plays a key role in the perception of the surrounding environment. In recent years, a myriad of processing methods [32, 43, 44, 70] have been proposed for efficient point cloud analysis, and their performances in applications, such as 3D point cloud classification [32, 43, 50, 56], seman-

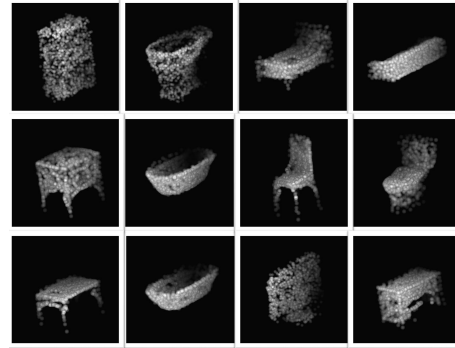


Figure 1. GDPNet performs point cloud classification and generation with a single network. It can generate 10 categories of point clouds, while achieving a 92.8% classification accuracy on ModelNet10. Sample point clouds generated by GDPNet are provided above.

tic segmentation [28, 31, 34, 47, 51, 52] and reconstruction [1, 15, 69, 71], have been improved significantly. Despite the significant progress of discriminative models for point cloud classification and segmentation, the research of generative models for point clouds is still far behind the discriminative ones. Learning generative models for point clouds is crucial to characterize the data distribution and analyze point clouds, which lays the foundation for various tasks such as shape completion, upsampling, synthesis and data augmentation. Although generative models such as variational auto-encoders (VAEs) [25] and generative adversarial networks (GANs) [11] have shown great success in 2D image generation, it is challenging to extend these well-established methods to unordered 3D point sets. Images are structured data on 2D grids, while point clouds lie in irregular 3D space with variable densities. Existing methods for point cloud generation are mainly based on volumetric data, e.g., 3D GAN [55], Generative VoxelNet [61, 64], 3D-INN [19], PointGrow [48], etc. While remarkable progress has been made, these methods have a few inherent limitations for point cloud generation. For instance,

the training procedure of GAN-based approaches [55] is rather unstable due to the adversarial losses, and the autoregressive models [48] assume an order of point generation, which is unnatural for orderless point cloud generation and restricts the modeling flexibility.

Energy-based models (EBMs) [29, 73] is a family of probabilistic generative models that can explicitly characterize the data distribution by learning an energy function that assigns lower values to observed data and higher values to unobserved ones. Besides, the training of EBMs can be much more stable in contrast to GANs by unifying representation and generation in one single model optimized by the maximum likelihood principle. Successful applications of EBMs include generations of images [59, 63], videos [60, 62], 3D volumetric shapes [61, 64], texts [6], molecules [21] as well as image-to-image translation [66] and out-of-distribution detection [33]. Recently, Xie et al. [65] propose GPointNet, an EBM for unordered point cloud generation. Unlike models that leverage an encoder-decoder architecture for generation, GPointNet [65] does not rely on either an auxiliary network or hand-crafted distance metrics to train the model. By incorporating PointNet [42], GPointNet extracts the features for each point independently and aggregates the point features from the whole point cloud into an energy scalar. The "fake" examples are then generated by the Langevin dynamics sampling [54], and the model parameters are updated based on the energy difference between the "fake" examples and the "real" observed examples in order to match the "fake" examples to the "real" ones in terms of some permutation-invariant statistical properties enabled by the energy function. Despite the model achieving an impressive performance for point cloud generation, one model needs to be trained separately for each category without sharing statistical regularities among different point cloud categories, e.g., structural smoothness and point density transition. Besides, their method is unable to classify point clouds directly and requires additional fine-tuning with an SVM classifier for classification.

In this paper, we propose GDPNet, the first hybrid Generative and Discriminative PointNet for point cloud classification and generation with a single network. Our design follows the framework of joint energy-based model (JEM) [13], which reinterprets CNN softmax classifier as an EBM for image classification and generation. Instead, we extend JEM for point cloud classification and generation based on a modern PointNet classifier [42]. The direct extension of JEM to PointNet, however, does not perform well as manifested by a classification accuracy gap to the standard classifier and a generation quality gap to the state-of-the-art generative approaches. We therefore investigate training techniques to bridge both gaps of GDPNet. We leverage the Sharpness-Aware Minimization (SAM) [8] to

improve the generalization of GDPNet (Section 3.2). We further demonstrate that the smoothness of the activation function can improve the training stability and synthesis quality of GDPNet significantly. As a result, our GDPNet retains strong discriminative power of modern PointNet classifier, while generating point cloud samples rivaling state-of-the-art generative approaches. More importantly, GDPNet yields one single model for classification and generation for all point cloud categories without resorting to a dedicated model for each category or additional fine-tuning step for classification. Example point clouds generated by GDPNet are provided in Figure 1.

## 2. Related Work

### 2.1. Deep Learning on Point Clouds

Following the breakthrough results of CNNs in 2D image processing tasks [16, 26], there has been a strong interest in adapting such methods to 3D geometric data. Compared to 2D images, point cloud data are sparse, unordered and locality-sensitive, making it non-trivial to adapt CNNs to point cloud processing. Early attempts focus on regular representations of the data in the form of 3D voxels [41, 58]. These methods quantize point clouds into regular voxels in 3D space with a predefined resolution and then apply volumetric convolution. Recently, new designs of local aggregators over point clouds are proposed to improve the efficiency of point cloud processing and reduce the loss of details [42, 43, 52]. PointNet [42] is a pioneer in deep architecture design that directly processes point clouds for classification and semantic segmentation by a shared multi-layer perception (MLP) and a max-pooling layer. However, it treats each point independently and ignores the geometric relationships among them, and thus only local features are extracted. PointNet++ [43] further introduces a hierarchical aggregation of point features to extract global features. In later works, DGCNN [52] proposes an effective EdgeConv that encodes the point relationships as edge features to better capture local geometric features, while still maintaining permutation-invariance. Our GDPNet reinterprets PointNet classifier as an EBM and empowers it for point cloud generation while retaining its strong discriminative power.

### 2.2. Point Cloud Generation

Since point clouds lie in irregular 3D space with variable densities, early point cloud generation methods [1, 9] convert the point cloud generation into a matrix generation problem. They take advantage of the power of well-established frameworks of variational auto-encoders (VAEs) [25] and generative adversarial networks (GANs) [11] to train generative models with hand-crafted distance metrics, such as Chamfer distance or earth mover's distance, to measure the dissimilarity of two point clouds.

The main defect of these methods is that they are restricted to generating point clouds with a fixed number of points and lack the property of permutation-invariance. FoldingNet [69] and AtlasNet [14] learn a mapping that deforms the 2D patches into 3D shapes of point clouds to generate an arbitrary number of points, while being permutation-invariant. On the other hand, point clouds can also be regarded as samples from a point distribution and the maximum likelihood principle can be utilized for point cloud generation. PointFlow [67] employs continuous normalizing flows [12] to model the distribution of points. The invertibility of normalizing flows enables the computation of the likelihood during training and the variational inference is adopted for model training. PointGrow [48] is an auto-regressive model that dynamically aggregates long-range dependencies among points for point cloud generation. ShapeGF [4] proposes a score-matching energy-based model to represent the distribution of points. Luo and Hu [35] view points in a point cloud as particles in a thermodynamic system that diffuse from the original distribution to a noise distribution and leverage the reverse diffusion Markov chain to model the distribution of points. GPointNet [65] explicitly models this distribution as an EBM and learns the model by the maximum likelihood estimation. However, all these methods focus on point cloud generation and cannot perform classification at the same time. To the best of our knowledge, our GDPNet is the first hybrid generative and discriminative model for point cloud classification and generation with a single network.

### 2.3. Flat Minima and Generalization

A great number of prior works have investigated the relationship between the flatness of local minima and the generalization of learned models [5, 8, 23, 27, 30, 53]. Now it is widely accepted and empirically verified that flat minima tend to give better generalization performance. Based on these observations, several recent regularization techniques are proposed to search for the flat minima of loss landscapes [5, 8, 27, 53]. Among them, the Sharpness-Aware Minimization (SAM) [8] is a recently introduced optimizer that demonstrates promising performance across all kinds of models and tasks, such as ResNet [17], Vision Transformer [5] and Language Models [2]. Furthermore, score matching-based methods [20, 45, 46, 49] also explore the behavior of flat minima in generative models and learn unnormalized statistical models by matching the gradient of the log probability density of model distribution to that of data distribution. Our GDPNet incorporates SAM to promote the energy landscape smoothness and thus improves the generalization of trained EBMs.

## 3. The Proposed Method

We first introduce the Joint Energy-based Models (JEM) [13] and discuss its extension to GDPNet, the first hybrid generative and discriminative model for point clouds. We then present the Sharpness-Aware-Minimization (SAM) [8] and its integration to GDPNet to improve the generalization of trained EBMs.

### 3.1. Joint Energy-based Models for Point Clouds

Let  $\mathbf{X} = \{\mathbf{x}_i \in \mathcal{R}^3\}_{i=1}^n$  denote a point cloud that contains  $n$  points, with  $\mathbf{x}_i$  representing the 3D coordinates of point  $i$ . Following the framework of Energy-Based Models (EBMs) [29, 73], we define the probability density function of a point cloud  $\mathbf{X}$  explicitly as

$$p_{\theta}(\mathbf{X}) = \frac{\exp(-E_{\theta}(\mathbf{X}))}{Z(\theta)}, \quad (1)$$

where  $E_{\theta}(\mathbf{X})$  is an energy function, parameterized by  $\theta$ , that maps input point cloud  $\mathbf{X}$  to a scalar, and  $Z(\theta) = \int_{\mathbf{X}} \exp(-E_{\theta}(\mathbf{X}))$  is the normalizing constant w.r.t.  $\mathbf{X}$  (also known as the partition function). Ideally, the energy function should assign low energy values to the samples drawn from data distribution, and high values otherwise. Since point cloud  $\mathbf{X}$  is a set of unordered points, the energy function,  $E_{\theta}(\mathbf{X})$ , defined on a point set needs to be invariant to the permutation of points in the set  $\mathbf{X}$ . We follow the design of PointNet [42] to employ a shared multi-layer perception (MLP) for each point in the set  $\mathbf{X}$ , followed by an average-pooling layer, to approximate a continuous set function to process the unordered point sets.

The maximum likelihood estimate (MLE) can be used to estimate parameters  $\theta$  of  $E_{\theta}(\mathbf{X})$ . However, since the partition function  $Z(\theta)$  is intractable, the MLE of  $\theta$  is not straightforward. Specifically, the derivative of the log-likelihood of  $\mathbf{X}$  w.r.t.  $\theta$  can be expressed as

$$\frac{\partial \log p_{\theta}(\mathbf{X})}{\partial \theta} = \mathbb{E}_{p_{\theta}(\mathbf{X})} \left[ \frac{\partial E_{\theta}(\mathbf{X})}{\partial \theta} \right] - \mathbb{E}_{p_d(\mathbf{X})} \left[ \frac{\partial E_{\theta}(\mathbf{X})}{\partial \theta} \right], \quad (2)$$

where  $p_d(\mathbf{X})$  is the real data distribution (i.e., training dataset), and  $p_{\theta}(\mathbf{X})$  is the estimated probability density function (1), sampling from which is challenging due to the intractable  $Z(\theta)$ .

Prior works have developed a number of methods to sample from  $p_{\theta}(\mathbf{X})$  efficiently, such as MCMC and Gibbs sampling [18]. To speed up the sampling process further, recently Stochastic Gradient Langevin Dynamics (SGLD) [54] has been employed to sample from  $p_{\theta}(\mathbf{X})$  by utilizing the gradient information [7, 13, 38]. Specifically, to sample from  $p_{\theta}(\mathbf{X})$ , SGLD follows

$$\mathbf{X}^0 \sim p_0(\mathbf{X}), \quad \mathbf{X}^{t+1} = \mathbf{X}^t - \frac{\alpha}{2} \frac{\partial E_{\theta}(\mathbf{X}^t)}{\partial \mathbf{X}^t} + \alpha \epsilon^t, \quad (3)$$

where  $\epsilon^t$  is random noise that is sampled from a unit Gaussian distribution  $\mathcal{N}(\mathbf{0}, \mathbf{1})$ , and  $p_0(\mathbf{X})$  is typically a uniform distribution over  $[-1, 1]$ , whose samples are refined via a noisy gradient decent with step-size  $\alpha$  over a sampling chain.

In order to train a hybrid generative and discriminative model, Joint Energy-based Model (JEM) [13] reinterprets the standard softmax classifier as an EBM. In particular, the logits  $f_\theta(\mathbf{X})[y]$  from a standard softmax classifier can be considered as an energy function over  $(\mathbf{X}, y)$ , where  $y$  is class label, and thus the joint density function of  $(\mathbf{X}, y)$  can be expressed as  $p_\theta(\mathbf{X}, y) = e^{f_\theta(\mathbf{X})[y]} / Z(\theta)$ , where  $Z(\theta)$  is an unknown normalizing constant (regardless of  $\mathbf{X}$  or  $y$ ). Then the density of  $\mathbf{X}$  can be derived by marginalizing over  $y$ :  $p_\theta(\mathbf{X}) = \sum_y p_\theta(\mathbf{X}, y) = \sum_y e^{f_\theta(\mathbf{X})[y]} / Z(\theta)$ . Subsequently, the corresponding energy function of  $\mathbf{X}$  can be identified as

$$E_\theta(\mathbf{X}) = -\log \sum_y \exp(f_\theta(\mathbf{X})[y]) = -\text{LSE}(f_\theta(\mathbf{X})), \quad (4)$$

where  $\text{LSE}(\cdot)$  denotes the Log-Sum-Exp function.

To optimize the model parameter  $\theta$ , JEM maximizes the logarithm of joint density function  $p_\theta(\mathbf{X}, y)$ :

$$\log p_\theta(\mathbf{X}, y) = \log p_\theta(y|\mathbf{X}) + \log p_\theta(\mathbf{X}), \quad (5)$$

where the first term denotes the cross-entropy objective for classification, and the second term can be optimized by the maximum likelihood learning of EBM as shown in Eq. (2). Sharing the same objective function (5) with JEM, GDPNet optimizes a single PointNet backbone for point cloud classification and generation. The overview of GDPNet is depicted in Figure 2.

### 3.2. Sharpness-Aware Minimization

The direct extension of JEM to PointNet above does not perform very well as manifested in our empirical studies (Tables 2, 3). In general, we notice two performance gaps of GDPNet as compared to the standard PointNet classifier and state-of-the-art generative approaches, i.e., a classification accuracy gap and a generation quality gap. We therefore investigate training techniques to bridge both gaps of GDPNet. In particular, we leverage the Sharpness-Aware Minimization (SAM) [8] to improve the generalization of GDPNet.

SAM [8] is a recently proposed optimization method that searches for model parameters  $\theta$  whose entire neighborhoods have uniformly low loss values by optimizing a minimax objective:

$$\min_{\theta} \max_{\|\epsilon\|_2 \leq \rho} L_{train}(\theta + \epsilon) + \lambda \|\theta\|_2^2, \quad (6)$$

where  $\rho$  is the radius of an  $L_2$ -ball centered at model parameter  $\theta$ , and  $\lambda$  is a hyperparameter for  $L_2$  regularization

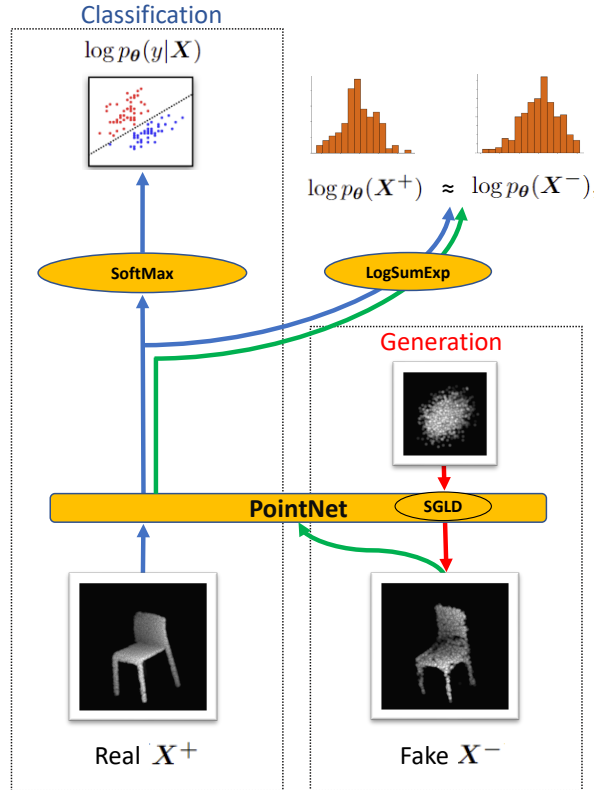


Figure 2. Overview of GDPNet architecture. Following the design of JEM [13], PointNet is leveraged for unordered point set feature extraction, and the  $\text{LogSumExp}(\cdot)$  of the logits from the softmax classifier can be re-used to define an energy function of point cloud  $\mathbf{X}$ , which leads to a hybrid generative and discriminative model with the fake samples generated from the SGLD sampling. The model is optimized to perform the classification and maximize the energy difference between fake and real samples.

on  $\theta$ . To solve the inner maximization problem, SAM employs the Taylor expansion to develop an efficient first-order approximation to the optimal  $\epsilon^*$  as:

$$\begin{aligned} \hat{\epsilon}(\theta) &= \arg \max_{\|\epsilon\|_2 \leq \rho} L_{train}(\theta) + \epsilon^T \nabla_{\theta} L_{train}(\theta) \\ &= \rho \nabla_{\theta} L_{train}(\theta) / \|\nabla_{\theta} L_{train}(\theta)\|_2, \end{aligned} \quad (7)$$

which is a scaled  $L_2$  normalized gradient at the current model parameters  $\theta$ . After  $\hat{\epsilon}$  is determined, SAM updates  $\theta$  based on the gradient  $\nabla_{\theta} L_{train}(\theta)|_{\theta + \hat{\epsilon}(\theta)} + 2\lambda\theta$  at an updated parameter location  $\theta + \hat{\epsilon}$ .

We incorporate SAM into the original training pipeline of GDPNet in order to improve the generalization of trained EBMs. Specifically, instead of the traditional maximum likelihood training of objective (5), we optimize the joint density function in a minimax objective:

$$\max_{\theta} \min_{\|\epsilon\|_2 \leq \rho} \log p_{(\theta + \epsilon)}(\mathbf{X}, y) - \lambda \|\theta\|_2^2. \quad (8)$$

---

**Algorithm 1** GDPNet training: Given network  $f_\theta$ , SGLD step-size  $\alpha$ , SGLD noise  $\sigma$ , SGLD steps  $K$ , replay buffer  $B$ , reinitialization frequency  $\gamma$ , SAM noise bound  $\rho$ , and learning rate  $lr$

---

```

1: while not converged do
2:   Sample  $\mathbf{X}^+$  and  $y$  from training dataset
3:   Sample  $\widehat{\mathbf{X}}_0 \sim B$  with probability  $1 - \gamma$ , else  $\widehat{\mathbf{X}}_0 \sim p_0(\mathbf{X})$ 
4:   for  $t = 1, 2, \dots, K$  do
5:      $\widehat{\mathbf{X}}_t = \widehat{\mathbf{X}}_{t-1} - \alpha \cdot \frac{\partial E(\widehat{\mathbf{X}}_{t-1})}{\partial \widehat{\mathbf{X}}_{t-1}} + \sigma \cdot \mathcal{N}(0, I)$ 
6:   end for
7:    $\mathbf{X}^- = \text{StopGrad}(\widehat{\mathbf{X}}_K)$ 
8:    $L_{\text{gen}}(\theta) = E(\mathbf{X}^+) - E(\mathbf{X}^-)$ 
9:    $L(\theta) = L_{\text{clf}}(\theta) + L_{\text{gen}}(\theta)$  with  $L_{\text{clf}}(\theta) = \text{xent}(f_\theta(\mathbf{X}^+), y)$ 
10:  # Apply SAM optimizer as follows:
11:  Compute gradient  $\nabla_\theta L(\theta)$  of the training loss
12:  Compute  $\hat{\epsilon}(\theta)$  with  $\rho$  as in Eq. (7)
13:  Compute gradient  $\mathbf{g} = \nabla_\theta L(\theta)|_{\theta+\epsilon(\theta)}$ 
14:  Update model parameters:  $\theta = \theta - lr \cdot \mathbf{g}$ 
15:  Add  $\mathbf{X}^-$  to  $B$ 
16: end while

```

---

For the outer maximization that involves  $\log p_\theta(\mathbf{X})$ , SGLD is again used to sample from  $p_\theta(\mathbf{X})$  as in the original JEM.

### 3.3. Smooth Activation Functions

We further study the effect of the activation function used in the energy function  $E_\theta(\mathbf{X})$ . Zhao et al. [72] demonstrate that when data  $\mathbf{X}$  is continuous, the smoothness of the activation function will substantially affect the Langevin sampling process (because the derivative  $\frac{\partial E_\theta(\mathbf{X})}{\partial \mathbf{X}}$  is inside of Eq. 3). Therefore, employing an activation function with continuous gradients everywhere can stabilize the sampling, while the non-smooth activation functions like ReLU [37] and LeakyReLU [36] may cause the divergence of EBM training. From our empirical studies, we have similar observations with the details provided in the experiments.

### 3.4. Training Algorithm

The pseudo-code of training GDPNet is provided in Algorithm 1, which follows a similar design of JEM [13] and JEM++ [68] with a replay buffer. For brevity, only one real sample and one generated sample are used to optimize the model parameter  $\theta$ . But it is straightforward to generalize the pseudo-code to a mini-batch setting, which we use in our experiments. It is worth mentioning that we adopt the Informative Initialization in JEM++ to initialize the Markov chain from  $p_0(\mathbf{X})$ , which enables batch normalization [22] in PointNet and plays a crucial role in the tradeoff between the number of SGLD sampling steps  $K$  and overall per-

formance, including the classification accuracy and training stability.

## 4. Experiments

We evaluate the classification and generation performance of GDPNet in this section, and compare it with standard PointNet classifier [42] and state-of-the-art generative models, including PointFlow [67] and GPointNet [65]. Ablation studies are performed to illustrate the impacts of SAM and smooth activation functions on the performance of GDPNet. Our source code is provided as a part of supplementary materials.

### 4.1. Experimental Setup

Our experiments largely follow the setup of GPointNet [65], and evaluate GDPNet for point cloud classification and generation on ModelNet10, which is a 10-category subset of ModelNet [57]. We first create a dataset from ModelNet10 by sampling 2,048 points uniformly from the mesh surface of each object and then scale the point cloud features to the range of [-1, 1]. In contrast to GPointNet [65], which trains 10 models to generate point clouds for 10 different categories of ModelNet10, we train one single network to classify and generate point clouds for all 10 categories.

For a fair comparison with GPointNet, PointNet [42] is used as the backbone network of our GDPNet. As discussed earlier, PointNet is permutation-invariant and thus works well with unordered point sets. It first maps each point (i.e., 3-dimensional coordinates) of a point cloud to a 1,024-dimensional feature vector by an MLP, then leverages an average pooling layer to aggregate information from all the points to a 1,024-dimensional global feature vector to represent the point cloud. A softmax layer is then appended at the end of the network to yield the logits for the 10 categories, which are used for classification and to calculate the energy score via an LSE( $\cdot$ ) operator (Eq. 4).

Furthermore, GDPNet employs SAM [8] to improve the generalization of trained EBMs. In our experiments, we use Adam [24] as the base optimizer for SAM with an initial learning rate of 0.01,  $\beta_1 = 0.9$  and  $\beta_2 = 0.999$ . We set the learning rate decay multiplier to 0.2 for every 50 iterations. We adopt the informative initialization of JEM++ [68] to initialize the Markov chain from  $p_0(\mathbf{X})$ . The reinitialization frequency  $\gamma$  is set to 0.05, and the replay buffer size is set to 5000. With the informative initialization, the number of SGLD sampling steps  $K$  can be reduced significantly as compared to that of GPointNet [65]. In our experiments, we set  $K = 32$  with a step size  $\alpha = 0.05$ . To mitigate the exploding gradients in the SGLD sampling, we clip the gradient values to the range of [-1, 1] at each sampling step. We run 200 epochs for training with a minibatch size of 128.

	Model	JSD ( $\downarrow$ )	MMD ( $\downarrow$ )		Coverage ( $\uparrow$ )	
			CD	EMD	CD	EMD
night stand	r-GAN	2.679	1.163	2.394	50.00	38.37
	l-GAN	1.000	0.746	1.563	44.19	39.53
	PointFlow	<b>0.240</b>	0.888	1.451	55.81	39.53
	GPointNet	0.590	<b>0.692</b>	<b>1.148</b>	<b>59.30</b>	<b>61.63</b>
	Ours	0.3771	0.886	1.369	54.83	59.30
	Training Set	0.263	0.793	1.096	60.40	52.32
toilet	r-GAN	3.180	2.995	2.891	17.00	16.00
	l-GAN	1.253	1.258	1.481	21.00	28.00
	PointFlow	<b>0.362</b>	0.965	1.513	39.00	33.00
	GPointNet	0.386	<b>0.816</b>	<b>1.265</b>	<b>44.00</b>	37.00
	Ours	0.578	0.867	1.314	43.00	<b>42.00</b>
	Training Set	0.249	0.823	1.116	48.00	51.00
monitor	r-GAN	2.936	1.524	2.021	21.00	24.00
	l-GAN	1.653	0.915	1.349	28.00	27.00
	PointFlow	<b>0.326</b>	0.831	1.288	37.00	32.00
	GPointNet	0.780	0.803	1.213	40.00	38.00
	Ours	0.434	<b>0.535</b>	<b>1.029</b>	<b>52.00</b>	<b>46.00</b>
	Training Set	0.283	0.554	0.938	48.00	53.00
chair	r-GAN	2.772	1.709	2.164	23.00	28.00
	l-GAN	1.358	1.419	1.480	23.00	26.00
	PointFlow	<b>0.278</b>	0.965	1.322	42.00	51.00
	GPointNet	0.563	<b>0.889</b>	<b>1.280</b>	<b>56.00</b>	<b>57.00</b>
	Ours	0.387	0.909	1.361	44.00	50.00
	Training Set	0.365	0.858	1.190	54.00	59.00
bathtub	r-GAN	3.014	2.478	2.536	26.00	30.00
	l-GAN	0.928	0.865	1.324	32.00	38.00
	PointFlow	<b>0.350</b>	<b>0.593</b>	1.320	50.00	44.00
	GPointNet	0.460	0.660	<b>1.108</b>	<b>58.00</b>	<b>50.00</b>
	Ours	0.490	0.647	1.103	54.00	<b>50.00</b>
	Training Set	0.344	0.652	0.980	56.00	52.00
sofa	r-GAN	1.866	2.037	2.247	13.00	23.00
	l-GAN	0.681	0.631	<b>1.028</b>	43.00	44.00
	PointFlow	<b>0.244</b>	0.585	1.313	34.00	33.00
	GPointNet	0.647	<b>0.547</b>	1.089	39.00	45.00
	Ours	0.275	0.576	1.104	<b>45.00</b>	<b>46.00</b>
	Training Set	0.185	0.467	0.904	56.00	56.00
bed	r-GAN	1.973	1.250	2.441	27.00	21.00
	l-GAN	0.646	<b>0.539</b>	<b>0.992</b>	48.00	44.00
	PointFlow	<b>0.219</b>	0.544	1.230	<b>50.00</b>	35.00
	GPointNet	0.461	0.552	1.004	<b>50.00</b>	<b>50.00</b>
	Ours	0.240	0.540	1.088	45.00	41.00
	Training Set	0.169	0.516	0.927	57.00	55.00
table	r-GAN	3.801	3.714	2.625	8.00	14.00
	l-GAN	4.254	1.232	2.166	14.00	9.00
	PointFlow	1.044	1.630	1.535	16.00	29.00
	GPointNet	0.869	<b>0.640</b>	<b>1.000</b>	<b>44.00</b>	<b>37.00</b>
	Ours	<b>0.761</b>	1.085	1.299	38.00	33.00
	Training Set	0.703	1.218	1.182	31.00	38.00
desk	r-GAN	3.575	2.712	3.678	22.09	22.09
	l-GAN	2.233	1.139	2.345	38.37	25.58
	PointFlow	0.327	1.254	1.548	38.37	46.51
	GPointNet	0.454	1.223	1.567	<b>56.98</b>	<b>52.33</b>
	Ours	0.512	<b>1.077</b>	<b>1.486</b>	55.81	50.51
	Training Set	0.329	1.055	1.332	53.48	50.00
dresser	r-GAN	1.726	1.299	1.675	36.05	30.23
	l-GAN	0.648	0.642	1.010	45.35	43.02
	PointFlow	<b>0.270</b>	0.715	1.349	46.51	37.21
	GPointNet	0.457	<b>0.485</b>	<b>0.988</b>	<b>53.49</b>	<b>52.33</b>
	Ours	0.440	0.708	1.125	48.88	49.53
	Training Set	0.215	0.551	0.882	56.98	54.65

Table 1. Qualities of point cloud synthesis on ModelNet10 from different methods. In contrast to the state-of-the-art generative approaches, GDPNet only trains a single network to generate all the 10 categories of ModelNet10.  $\downarrow$ : the lower the better;  $\uparrow$ : the higher the better. MMD-CD scores are multiplied by 100; MMD-EMD scores and JSDs are multiplied by 10.

## 4.2. Evaluation Metrics

We adopt three evaluation metrics: Jensen-Shannon Divergence (JSD), Coverage (COV) and Minimum Matching Distance (MMD) to evaluate the quality of generated point clouds. These metrics are commonly used in prior works [1, 65, 67] for point cloud quality evaluation. When evaluating COV and MMD, we use Chamfer Distance (CD) and Earth Mover’s Distance (EMD) to measure the dissimilarity between two point clouds, which are defined formally as follows:

$$\text{CD}(X, Y) = \sum_{x \in X} \min_{y \in Y} \|x - y\|_2 + \sum_{y \in Y} \min_{x \in X} \|x - y\|_2,$$

$$\text{EMD}(X, Y) = \min_{\phi: X \rightarrow Y} \sum_{x \in X} \|x - \phi(x)\|_2,$$

where  $X$  and  $Y$  are two point clouds with the same number of points and  $\phi$  is a bijection between them.

**Jensen-Shannon Divergence (JSD)** is a symmetrized Kullback-Leibler divergence between two marginal point distributions:

$$\text{JSD}(P_g, P_r) = \frac{1}{2} D_{KL}(P_r \| M) + \frac{1}{2} D_{KL}(P_g \| M),$$

where  $M = \frac{1}{2}(P_r + P_g)$ ,  $P_r$  and  $P_g$  are marginal distributions of points in the reference and generated sets, approximated by discretizing the space into  $28^3$  voxels and assigning each point to one of them.

**Coverage (COV)** measures the fraction of point clouds in the reference set that are matched to at least one point cloud in the generated set. For each point cloud in the generated set, its nearest neighbor in the reference set is marked as a match:

$$\text{COV}(S_g, S_r) = \frac{|\{\arg \min_{Y \in S_r} D(X, Y) | X \in S_g\}|}{|S_r|},$$

where  $D(\cdot, \cdot)$  can be either CD or EMD.

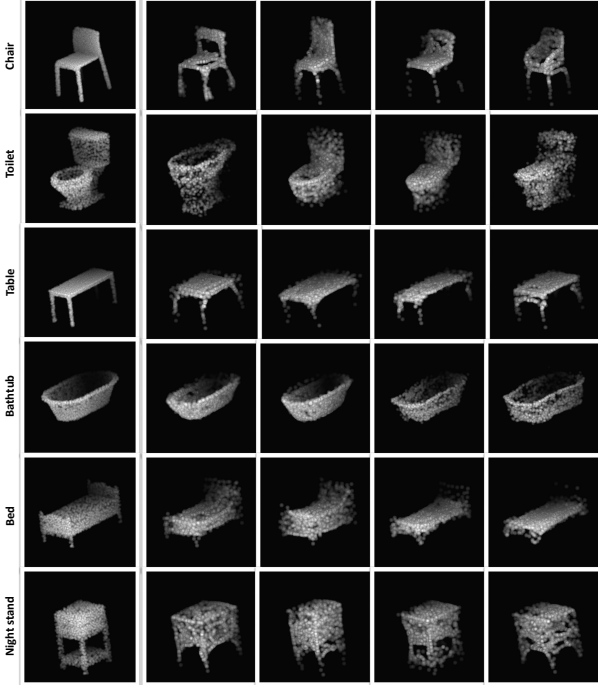


Figure 3. Sample point clouds generated by GDPNet. Each row corresponds to one category. The first column is a sample from ModelNet10 training set, and the rest of the columns are synthesized point clouds generated via SGLD.

**Minimum Matching Distance (MMD)** is proposed to complement coverage to measure the quality of generated point clouds. For each point cloud in the reference set, the distance to its nearest neighbor in the generated set is computed and averaged:

$$\text{MMD}(S_g, S_r) = \frac{1}{|S_r|} \sum_{Y \in S_r} \min_{X \in S_g} D(X, Y).$$

### 4.3. Results of Point Cloud Generation

We compare the generative performance of GDPNet with four baseline generative approaches: l-GAN [1], r-GAN [1], PointFlow [67] and GPointNet [65], and the results are reported in Table 1. It can be observed that GDPNet achieves a competitive generative performance as compared to the state-of-the-art results of PointFlow and GPointNet even though our method only employs a single network to generate point clouds from 10 different categories of ModelNet10<sup>1</sup>. For the generation of "monitor", GDPNet achieves an even better result than that of GPointNet, while being competitive with GPointNet for the rest of the categories. As shown in Figure 1, GDPNet can learn the complex distributions among all the categories and generate point clouds

<sup>1</sup>Let alone our GDPNet can also classify point cloud directly with an accuracy of 92.8%.

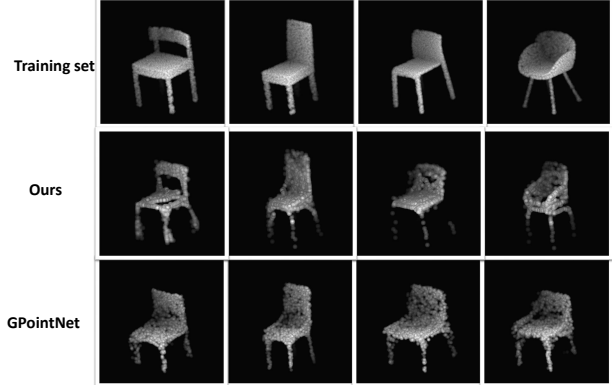


Figure 4. Sample point clouds generated by GPointNet [65] and GDPNet. Our GDPNet generates chairs with more diverse styles, while GPointNet generates chairs with better details on the four legs.

of each category with diverse styles. It also can generate point clouds that have features from multiple categories, such as a toilet-like chair. This is because toilet and chair share some similar features, and GDPNet can generate samples that interpolate between them.

Figure 3 provides more sample point clouds generated by GDPNet for categories of "chair", "toilet", "table", "bathtub", "bed" and "night stand". These samples are selected when the GDPNet classifier has a classification confidence over 90%. Not surprisingly, the generated samples for each category are exactly as GDPNet predicted, which also indicates an accurate classification of GDPNet. The results in Figure 3 show that GDPNet can learn the complex point distribution to generate quality point cloud samples. For "chair" and "table", the details of four legs are captured by our model, and the "bathtub" samples are as good as training samples, while the toilet samples are also decent. As for "night stand", whose shape is much more complex, the generated samples can still capture parts of the object features. We also used the official GPointNet checkpoint for the chair category to generate 1,000 samples, from which we selected some high-quality ones and compare them with the samples from our GDPNet. It can be observed from Figure 4 that GDPNet can generate chairs with more diverse styles, while GPointNet generates chairs with better details on the four legs. As a result, GDPNet has a slightly lower evaluation value on "chair" as reported in Table 1.

As for model complexity, GDPNet has a 1/10 model size of GPointNet since GDPNet only trains one single network to generate point clouds for all the 10 categories, which is a significant advantage of our method as compared to other generative approaches. For models based on VAEs or GANs, their model sizes are even larger than that of GPointNet as they need auxiliary networks for training.

	Method	JSD ( $\downarrow$ )	MMD ( $\downarrow$ )		Coverage ( $\uparrow$ )	
			CD	EMD	CD	EMD
Night Stand	ReLU	0.487	0.911	1.320	43.02	47.67
	CELU	<b>0.368</b>	<b>0.867</b>	<b>1.311</b>	53.48	54.65
	CELU + SAM	0.377	0.886	1.369	<b>54.83</b>	<b>59.30</b>
Toilet	ReLU	0.581	1.022	1.478	31.00	42.00
	CELU	<b>0.546</b>	0.941	1.380	32.00	37.00
	CELU + SAM	0.578	<b>0.867</b>	<b>1.314</b>	<b>43.00</b>	<b>42.00</b>
Monitor	ReLU	0.410	0.692	1.261	45.00	46.00
	CELU	<b>0.389</b>	0.571	1.085	46.00	44.00
	CELU + SAM	0.434	<b>0.535</b>	<b>1.029</b>	<b>52.00</b>	<b>46.00</b>
Chair	ReLU	0.449	0.916	1.495	44.00	46.00
	CeLU	<b>0.363</b>	<b>0.8541</b>	<b>1.316</b>	<b>45.00</b>	<b>51.00</b>
	CELU + SAM	0.387	0.909	1.361	44.00	50.00

Table 2. The impacts of SAM and activation functions on the qualities of generated point clouds by GDPNet.  $\downarrow$ : the lower the better;  $\uparrow$ : the higher the better. MMD-CD scores are multiplied by 100; MMD-EMD scores and JSDs are multiplied by 10.

#### 4.4. Ablation Studies

We study the impacts of SAM and the activation functions on the performance of GDPNet for point cloud classification and generation, respectively.

**Point cloud generation** Table 2 reports the impacts of SAM and activation functions to the generative performance of GDPNet. By replacing the popular ReLU activation function [37] with CELU [3], a continuously differentiable exponential linear unit, GDPNet achieves notable quality gains in generating point clouds of different categories. This observation is consistent with that of Zhao et al. [72] who demonstrate that the smoothness of the activation functions substantially improves the SGLD sampling process and thus the synthesis quality. Table 2 also shows that incorporating SAM to GDPNet does not improve the synthesis quality consistently. However, from our experiments, we find that SAM facilitates the convergence of the model, stabilizes the training of GDPNet, and improves the classification accuracy as shown in the experiments below.

**Point cloud classification** Table 3 reports the impacts of SAM and the activation functions on the classification performance of GDPNet. It can be observed that without SAM and CELU activation function, GDPNet has a non-competitive classification accuracy of 90.7% as compared to the standard PointNet classifier, which achieves a 92.8% accuracy. Incorporating SAM into GDPNet significantly improves the classification accuracy (92.8%), which matches with that of the standard PointNet classifier. Replacing CELU by ReLU in GDPNet does not affect the classification accuracy much (92.9% vs. 92.8%), but GDPNet with CELU achieves the best synthesis quality as shown in Table 2. Therefore, GDPNet with SAM and CELU bridges both the classification accuracy gap and the synthesis quality gap as compared to the standard PointNet classifier and state-of-the-art generative approaches.

It is worth mentioning that even though I-GAN [1], PointFlow [67] and GPointNet [65] achieve better classification accuracies as reported in Table 3. They can not classify point clouds directly since they are generative models. Specifically, to classify point clouds with GPointNet [65], an one-versus-all SVM classifier needs to be trained on the extracted features of GPointNet and the class labels. A similar procedure has also been used by I-GAN and PointFlow for classification. In contrast, GDPNet does not need any extra training step for classification, which is another significant advantage of GDPNet as compared to these generative approaches.

Method	Accuracy
I-GAN* [1]	95.4%
PointFlow* [67]	93.7%
GPointNet* [65]	93.7%
PointNet [42]	92.8%
GDPNet w/ ReLU - SAM	90.7%
GDPNet w/ ReLU	92.9%
GDPNet - SAM	90.3%
GDPNet	92.8%

Table 3. Point cloud classification accuracies on ModelNet10. \* denotes the method needs to train an SVM classifier on the extracted features for classification.

## 5. Conclusion

This paper introduces GDPNet, a hybrid generative and discriminative model for point clouds, that is based on joint energy-based models. GDPNet further leverages SAM and CELU activation function to bridge the classification accuracy gap and the generation quality gap to the standard PointNet classifier and state-of-the-art generative models. Compared to prior generative models of point clouds, GDPNet only trains a single compact network to classify and generate point clouds of all categories. Experi-



ments demonstrate our GDPNet retains strong discriminative power of modern PointNet classifiers, while generating point cloud samples rivaling state-of-the-art generative approaches. To the best of our knowledge, GDPNet is the first hybrid generative and discriminative model for point clouds.

## References

- [1] Panos Achlioptas, Olga Diamanti, Ioannis Mitliagkas, and Leonidas J. Guibas. Learning Representations and Generative Models For 3D Point Clouds. *Proceedings of the 35th International Conference on Machine Learning (ICML)*, pages 40–49, 2018. [1](#), [2](#), [6](#), [7](#), [8](#)
- [2] Dara Bahri, Hossein Mobahi, and Yi Tay. Sharpness-aware minimization improves language model generalization. In *Annual Meeting of the Association for Computational Linguistics (ACL)*, 2022. [3](#)
- [3] Jonathan T Barron. Continuously differentiable exponential linear units. *arXiv preprint arXiv:1704.07483*, 2017. [8](#)
- [4] Ruojin Cai, Guandao Yang, Hadar Averbuch-Elor, Zekun Hao, Serge Belongie, Noah Snavely, and Bharath Hariharan. Learning gradient fields for shape generation. In *European Conference on Computer Vision*, pages 364–381. Springer, 2020. [3](#)
- [5] Xiangning Chen, Cho-jui Hsieh, and Boqing Gong. When vision transformers outperform resnets without pre-training or strong data augmentations. In *International Conference on Learning Representations (ICLR)*, 2022. [3](#)
- [6] Yuntian Deng, Anton Bakhtin, Myle Ott, Arthur Szlam, and Marc’Aurelio Ranzato. Residual energy-based models for text generation. *arXiv preprint arXiv:2004.11714*, 2020. [2](#)
- [7] Yilun Du and Igor Mordatch. Implicit generation and generalization in energy-based models. In *Neural Information Processing Systems (NeurIPS)*, 2019. [3](#)
- [8] Pierre Foret, Ariel Kleiner, Hossein Mobahi, and Behnam Neyshabur. Sharpness-aware minimization for efficiently improving generalization. In *International Conference on Learning Representations*, 2021. [2](#), [3](#), [4](#), [5](#)
- [9] Matheus Gadelha, Rui Wang, and Subhransu Maji. Multiresolution tree networks for 3d point cloud processing. In *Proceedings of the European Conference on Computer Vision (ECCV)*, pages 103–118, 2018. [2](#)
- [10] Andreas Geiger, Philip Lenz, and Raquel Urtasun. Are we ready for autonomous driving? the kitti vision benchmark suite. In *2012 IEEE Conference on Computer Vision and Pattern Recognition*, pages 3354–3361, 2012. [1](#)
- [11] Ian Goodfellow, Jean Pouget-Abadie, Mehdi Mirza, Bing Xu, David Warde-Farley, Sherjil Ozair, Aaron Courville, and Yoshua Bengio. Generative adversarial nets. In *Neural Information Processing Systems (NeurIPS)*, 2014. [1](#), [2](#)
- [12] Will Grathwohl, Ricky T. Q. Chen, Jesse Bettencourt, Ilya Sutskever, and David Duvenaud. Ffjord: Free-form continuous dynamics for scalable reversible generative models. In *International Conference on Learning Representations (ICLR)*, 2019. [3](#)
- [13] Will Grathwohl, Kuan-Chieh Wang, Joern-Henrik Jacobsen, David Duvenaud, Mohammad Norouzi, and Kevin Swersky. Your classifier is secretly an energy based model and you should treat it like one. In *International Conference on Learning Representations (ICLR)*, 2020. [1](#), [2](#), [3](#), [4](#), [5](#)
- [14] Thibault Groueix, Matthew Fisher, Vladimir G Kim, Bryan C Russell, and Mathieu Aubry. A papier-mâché approach to learning 3d surface generation. In *Proceedings of the IEEE conference on computer vision and pattern recognition*, pages 216–224, 2018. [3](#)
- [15] Zhizhong Han, Xiyang Wang, Yu-Shen Liu, and Matthias Zwicker. Multi-Angle Point Cloud-VAE: Unsupervised Feature Learning for 3D Point Clouds from Multiple Angles by Joint Self-Reconstruction and Half-to-Half Prediction. *Proceedings of the International Conference on Computer Vision (ICCV)*, 2019. [1](#)
- [16] Kaiming He, Xiangyu Zhang, Shaoqing Ren, and Jian Sun. Deep residual learning for image recognition. In *Proceedings of the IEEE conference on computer vision and pattern recognition (CVPR)*, 2016. [2](#)
- [17] Kaiming He, Xiangyu Zhang, Shaoqing Ren, and Jian Sun. Deep residual learning for image recognition. In *IEEE Conference on Computer Vision and Pattern Recognition (CVPR)*, 2016. [3](#)
- [18] Geoffrey E Hinton. Training products of experts by minimizing contrastive divergence. *Neural computation*, 2002. [3](#)
- [19] Wenlong Huang, Brian Lai, Weijian Xu, and Zhuowen Tu. 3d volumetric modeling with introspective neural networks. In *Proceedings of the AAAI Conference on Artificial Intelligence*, pages 8481–8488, 2019. [1](#)
- [20] Aapo Hyvärinen. Estimation of non-normalized statistical models by score matching. *Journal of Machine Learning Research*, 2005. [3](#)
- [21] John Ingraham, Adam Riesselman, Chris Sander, and Debora Marks. Learning protein structure with a differentiable simulator. In *International Conference on Learning Representations*, 2018. [2](#)
- [22] Sergey Ioffe and Christian Szegedy. Batch normalization: Accelerating deep network training by reducing internal covariate shift. In *International Conference on Machine Learning (ICML)*, 2015. [5](#)
- [23] Nitish Shirish Keskar, Dheevatsa Mudigere, Jorge Nocedal, Mikhail Smelyanskiy, and Ping Tak Peter Tang. On large-batch training for deep learning: Generalization gap and sharp minima. In *International Conference on Learning Representations (ICLR)*, 2017. [3](#)
- [24] Diederik Kingma and Jimmy Ba. Adam: A method for stochastic optimization. In *International Conference on Learning Representations (ICLR)*, 2015. [5](#)
- [25] Diederik P Kingma and Max Welling. Auto-encoding variational bayes. In *International Conference on Learning Representations (ICLR)*, 2014. [1](#), [2](#)
- [26] Alex Krizhevsky, Ilya Sutskever, and Geoffrey E Hinton. Imagenet classification with deep convolutional neural networks. In *Advances in Neural Information Processing Systems (NeurIPS)*, 2012. [2](#)

- [27] Jungmin Kwon, Jeongseop Kim, Hyunseo Park, and In Kwon Choi. Asam: Adaptive sharpness-aware minimization for scale-invariant learning of deep neural networks. In *International Conference on Machine Learning (ICML)*, 2021. 3
- [28] Loic Landrieu and Martin Simonovsky. Large-scale Point Cloud Semantic Segmentation with Superpoint Graphs. *Proceedings of the IEEE Conference on Computer Vision and Pattern Recognition (CVPR)*, pages 4558–4567, 2018. 1
- [29] Yann LeCun, Sumit Chopra, Raia Hadsell, M Ranzato, and F Huang. A tutorial on energy-based learning. *Predicting structured data*, 2006. 2, 3
- [30] Hao Li, Zheng Xu, Gavin Taylor, Christoph Studer, and Tom Goldstein. Visualizing the Loss Landscape of Neural Nets. In *Neural Information Processing Systems (NeurIPS)*, 2018. 3
- [31] Jiaxin Li, Ben M Chen, and Gim Hee Lee. SO-Net: Self-Organizing Network for Point Cloud Analysis. *Proceedings of the IEEE Conference on Computer Vision and Pattern Recognition (CVPR)*, pages 9397–9406, 2018. 1
- [32] Yangyan Li, Rui Bu, Mingchao Sun, Wei Wu, Xinhan Di, and Baoquan Chen. PointCNN: Convolution On X-Transformed Points. *Proceedings of Advances in Neural Information Processing Systems (NeurIPS)*, 2018. 1
- [33] Weitang Liu, Xiaoyun Wang, John Owens, and Yixuan Li. Energy-based out-of-distribution detection. *Neural Information Processing Systems (NeurIPS)*, 2020. 2
- [34] Yongcheng Liu, Bin Fan, Shiming Xiang, and Chunhong Pan. Relation-Shape Convolutional Neural Network for Point Cloud Analysis. *Proceedings of the IEEE Conference on Computer Vision and Pattern Recognition (CVPR)*, pages 8895–8904, 2019. 1
- [35] Shitong Luo and Wei Hu. Diffusion probabilistic models for 3d point cloud generation. In *Proceedings of the IEEE/CVF Conference on Computer Vision and Pattern Recognition*, pages 2837–2845, 2021. 3
- [36] Andrew Maas, Awni Hannun, and Andrew Ng. Rectifier nonlinearities improve neural network acoustic models. In *International Conference on Machine Learning (ICML)*, 2013. 5
- [37] Vinod Nair and Geoffrey E Hinton. Rectified linear units improve restricted boltzmann machines. In *International Conference on Machine Learning (ICML)*, 2011. 5, 8
- [38] Erik Nijkamp, Song-Chun Zhu, and Ying Nian Wu. Learning non-convergent short-run mcmc toward energy-based model. In *Neural Information Processing Systems (NeurIPS)*, 2019. 3
- [39] Andreas Nüchter and Joachim Hertzberg. Towards semantic maps for mobile robots. *Robotics Auton. Syst.*, 56:915–926, 2008. 1
- [40] Youngmin Park, Vincent Lepetit, and Woontack Woo. Multiple 3d object tracking for augmented reality. In *2008 7th IEEE/ACM International Symposium on Mixed and Augmented Reality*, pages 117–120, 2008. 1
- [41] Charles R. Qi, Hao Su, Matthias Nießner, Angela Dai, Mengyuan Yan, and Leonidas J. Guibas. Volumetric and Multi-View CNNs for Object Classification on 3D Data. *Proceedings of the IEEE Conference on Computer Vision and Pattern Recognition (CVPR)*, pages 5648–5656, 2016. 2
- [42] Charles R. Qi, Hao Su, Kaichun Mo, and Leonidas J. Guibas. PointNet: Deep Learning on Point Sets for 3D Classification and Segmentation. *Proceedings of the IEEE Conference on Computer Vision and Pattern Recognition (CVPR)*, pages 652–660, 2017. 1, 2, 3, 5, 8
- [43] Charles R. Qi, Li Yi, Hao Su, and Leonidas J. Guibas. PointNet++: Deep Hierarchical Feature Learning on Point Sets in a Metric Space. *Proceedings of Advances in Neural Information Processing Systems (NeurIPS)*, 2017. 1, 2
- [44] Charles R. Qi, Or Litany, Kaiming He, and Leonidas J. Guibas. Deep Hough Voting for 3D Object Detection in Point Clouds. *Proceedings of the International Conference on Computer Vision (ICCV)*, 2019. 1
- [45] Yang Song and Stefano Ermon. Generative modeling by estimating gradients of the data distribution. In *Neural Information Processing Systems (NeurIPS)*, 2019. 3
- [46] Yang Song, Jascha Sohl-Dickstein, Diederik P Kingma, Abhishek Kumar, Stefano Ermon, and Ben Poole. Score-based generative modeling through stochastic differential equations. In *International Conference on Learning Representations*, 2020. 3
- [47] Hang Su, Varun Jampani, Deqing Sun, Subhransu Maji, Evangelos Kalogerakis, Ming-Hsuan Yang, and Jan Kautz. SPLATNet: Sparse Lattice Networks for Point Cloud Processing. *Proceedings of the IEEE Conference on Computer Vision and Pattern Recognition (CVPR)*, pages 2530–2539, 2018. 1
- [48] Yongbin Sun, Yue Wang, Ziwei Liu, Joshua Siegel, and Sanjay Sarma. Pointgrow: Autoregressively learned point cloud generation with self-attention. In *Proceedings of the IEEE/CVF Winter Conference on Applications of Computer Vision*, pages 61–70, 2020. 1, 2, 3
- [49] Kevin Swersky, David Buchman, Nando D Freitas, Benjamin M Marlin, et al. On autoencoders and score matching for energy based models. In *International Conference on Machine Learning (ICML)*, 2011. 3
- [50] Hugues Thomas, Charles R. Qi, Jean-Emmanuel Deschaud, Beatriz Marcotegui, François Goulette, and Leonidas J. Guibas. KPConv: Flexible and Deformable Convolution for Point Clouds. *Proceedings of the IEEE International Conference on Computer Vision (ICCV)*, 2019. 1
- [51] Weiyue Wang, Ronald Yu, Qiangui Huang, and Ulrich Neumann. SGPN: Similarity Group Proposal Network for 3D Point Cloud Instance Segmentation. *Proceedings of the IEEE Conference on Computer Vision and Pattern Recognition (CVPR)*, pages 2569–2578, 2018. 1
- [52] Yue Wang, Yongbin Sun, Ziwei Liu, Sanjay E. Sarma, Michael M. Bronstein, and Justin M. Solomon. Dynamic Graph CNN for Learning on Point Clouds. *ACM Transactions on Graphics (TOG)*, 2019. 1, 2
- [53] Colin Wei, Sham Kakade, and Tengyu Ma. The implicit and explicit regularization effects of dropout. In *International Conference on Machine Learning (ICML)*, 2020. 3

- [54] Max Welling and Yee W Teh. Bayesian learning via stochastic gradient langevin dynamics. In *International Conference on Machine Learning (ICML)*, 2011. [2](#), [3](#)
- [55] Jiajun Wu, Chengkai Zhang, Tianfan Xue, Bill Freeman, and Josh Tenenbaum. Learning a probabilistic latent space of object shapes via 3d generative-adversarial modeling. *Advances in neural information processing systems*, 29, 2016. [1](#), [2](#)
- [56] Wenxuan Wu, Zhongang Qi, and Li Fuxin. PointConv: Deep Convolutional Networks on 3D Point Clouds. *Proceedings of the IEEE Conference on Computer Vision and Pattern Recognition (CVPR)*, pages 9622–9630, 2019. [1](#)
- [57] Zhirong Wu, S. Song, A. Khosla, Fisher Yu, Linguang Zhang, Xiaoou Tang, and J. Xiao. 3d shapenets: A deep representation for volumetric shapes. In *2015 IEEE Conference on Computer Vision and Pattern Recognition (CVPR)*, pages 1912–1920, Los Alamitos, CA, USA, 2015. IEEE Computer Society. [5](#)
- [58] Z. Wu, S. Song, A. Khosla, F. Yu, L. Zhang, X. Tang, and J. Xiao. 3D ShapeNets: A Deep Representation for Volumetric Shapes. *Proceedings of the IEEE Conference on Computer Vision and Pattern Recognition (CVPR)*, pages 1912–1920, 2015. [2](#)
- [59] Jianwen Xie, Yang Lu, Song-Chun Zhu, and Yingnian Wu. A theory of generative convnet. In *International Conference on Machine Learning (ICML)*, 2016. [2](#)
- [60] Jianwen Xie, Song-Chun Zhu, and Ying Nian Wu. Synthesizing dynamic patterns by spatial-temporal generative convnet. In *Proceedings of the IEEE conference on computer vision and pattern recognition*, pages 7093–7101, 2017. [2](#)
- [61] Jianwen Xie, Zilong Zheng, Ruiqi Gao, Wenguan Wang, Song-Chun Zhu, and Ying Nian Wu. Learning descriptor networks for 3d shape synthesis and analysis. In *Proceedings of the IEEE conference on computer vision and pattern recognition*, pages 8629–8638, 2018. [1](#), [2](#)
- [62] Jianwen Xie, Song-Chun Zhu, and Ying Nian Wu. Learning energy-based spatial-temporal generative convnets for dynamic patterns. *IEEE transactions on pattern analysis and machine intelligence*, 43(2):516–531, 2019. [2](#)
- [63] Jianwen Xie, Yang Lu, Ruiqi Gao, Song-Chun Zhu, and Ying Nian Wu. Cooperative training of descriptor and generator networks. *IEEE Transactions on Pattern Analysis and Machine Intelligence*, 2020. [2](#)
- [64] Jianwen Xie, Zilong Zheng, Ruiqi Gao, Wenguan Wang, Song-Chun Zhu, and Ying Nian Wu. Generative voxelnet: learning energy-based models for 3d shape synthesis and analysis. *IEEE Transactions on Pattern Analysis and Machine Intelligence*, 2020. [1](#), [2](#)
- [65] Jianwen Xie, Yifei Xu, Zilong Zheng, Song-Chun Zhu, and Ying Nian Wu. Generative pointnet: Deep energy-based learning on unordered point sets for 3d generation, reconstruction and classification. In *Proceedings of the IEEE/CVF Conference on Computer Vision and Pattern Recognition*, pages 14976–14985, 2021. [1](#), [2](#), [3](#), [5](#), [6](#), [7](#), [8](#)
- [66] Jianwen Xie, Zilong Zheng, Xiaolin Fang, Song-Chun Zhu, and Ying Nian Wu. Cooperative training of fast thinking initializer and slow thinking solver for conditional learning. *IEEE Transactions on Pattern Analysis and Machine Intelligence*, 2021. [2](#)
- [67] Guandao Yang, Xun Huang, Zekun Hao, Ming-Yu Liu, Serge Belongie, and Bharath Hariharan. PointFlow: 3D Point Cloud Generation with Continuous Normalizing Flows. *Proceedings of the IEEE International Conference on Computer Vision (ICCV)*, 2019. [3](#), [5](#), [6](#), [7](#), [8](#)
- [68] Xiulong Yang and Shihao Ji. JEM++: Improved Techniques for Training JEM. In *International Conference on Computer Vision (ICCV)*, 2021. [1](#), [5](#)
- [69] Yaoqing Yang, Chen Feng, Yiru Shen, and Dong Tian. FoldingNet: Point Cloud Auto-encoder via Deep Grid Deformation. *Proceedings of the IEEE Conference on Computer Vision and Pattern Recognition (CVPR)*, pages 206–215, 2018. [1](#), [3](#)
- [70] Lequan Yu, Xianzhi Li, Chi-Wing Fu, Daniel Cohen-Or, and Pheng Ann Heng. PU-Net: Point Cloud Upsampling Network. *Proceedings of IEEE Conference on Computer Vision and Pattern Recognition (CVPR)*, pages 2790–2799, 2018. [1](#)
- [71] Yongheng Zhao, Tolga Birdal, Haowen Deng, and Federico Tombari. 3D Point-Capsule Networks. *Proceedings of the IEEE Conference on Computer Vision and Pattern Recognition (CVPR)*, pages 1009–1018, 2019. [1](#)
- [72] Yang Zhao, Jianwen Xie, and Ping Li. Learning energy-based generative models via coarse-to-fine expanding and sampling. In *International Conference on Learning Representations ICLR*, 2021. [5](#), [8](#)
- [73] Song Chun Zhu, Yingnian Wu, and David Mumford. Filters, random fields and maximum entropy (frame): Towards a unified theory for texture modeling. *International Journal of Computer Vision*, 27(2):107–126, 1998. [2](#), [3](#)